Visible Light Positioning using an Aperture and a Quadrant Photodiode

Stefanie Cincotta, Adrian Neild, Cuiwei He and Jean Armstrong
Monash University,
Melbourne, Australia
{Stefanie.Cincotta, Adrian.Neild, Cuiwei.He, Jean.Armstrong}@monash.edu

***Abstract*— This paper describes a new form of angle of arrival (AOA) detector which can be applied in an indoor visible light positioning system using LED luminaires. In this new detector, a quadrant photodiode (PD) is placed below a transparent aperture in an opaque screen. Light passing through the aperture creates an illuminated area on the quadrant PD. This light spot has the same shape and size as the aperture. The position of the light spot on the PD depends on the AOA of the light. It is shown that this position can be determined by measuring the relative optical power of the light reaching each of the four quadrants of the PD. For the case of a square aperture and a square photodetector, a simple algorithm can be used to determine the *x* and *y* coordinates of the center of the light spot on the PD. From this, the AOA can be calculated. Simulations for an indoor visible light positioning system using LED luminaires and realistic parameters show that accurate AOA estimation is possible. If different luminaires transmit different orthogonal signals, digital signal processing can be used to separately estimate the received signal powers from each of the transmitting luminaires. Thus, this new detector has the potential to provide accurate three-dimensional positioning using a single quadrant PD.**

Keywords—Indoor Positioning, Visible Light, VLP, Quadrant photodiode, Aperture, ADA receiver

I. INTRODUCTION

Visible light positioning (VLP) and visible light communications (VLC) are emerging as important new technologies that use LED luminaires to transmit signals which can be used for positioning [1] or communications [2]. The VLP systems described to date have used two broad classes of receivers; those using a general purpose camera to detect the light signals and those using separate photodiodes (PDs). While a number of innovative camera based systems have been described [3], [4], their performance is limited by a combination of the limited frame rate of the camera and the requirement for the frequency of signals transmitted by the luminaires to be above the flicker level [5]. PD based systems do not face this limitation.

In a typical VLP system, each LED luminaire transmits a signal which contains information about the position of the luminaire within a room. Based on properties of the received signals, the receiver can determine its relative distance or direction from the luminaire. Many different VLP approaches have been described in the literature, including those based on received signal strength (RSS) [6], time of arrival (TOA) [7], time difference of arrival (TDOA) [8], fingerprinting [9], angle of arrival (AOA) [10] and other techniques [11]. The different approaches have various advantages and disadvantages. RSS systems estimate the distance from the receiver to the transmitter based on the measured RSS and knowledge of the transmitted power and radiation pattern of the transmitter. As such, while conceptually simple, RSS techniques are vulnerable to changes in transmitted power caused by practical aspects such as aging of the LEDs or even an accumulation of dust on the luminaire. TOA and TDOA depend on accurate synchronization and accurate measurement of very small time intervals. Properties that are unlikely to be achieved in consumer products. The use of AOA has many advantages, as the position of the transmitters and hence the AOA of light at a given receiver position does not change over time. However, the major challenge for AOA systems using PDs is to design compact AOA receivers. For VLP to achieve widespread adoption, receivers will have to be incorporated in devices such as smart phones.

A number of papers have described receivers which show that accurate AOA positioning systems can be designed, but most of these have used PDs mounted on three dimensional structures such as pyramids [12] or cubes [13]. However, these are incompatible with incorporation in a smart phone as they have a protruding structure which would be unacceptable to consumers. If they were modified to have a recessed structure, this would limit the overall field of view (FOV). This restricted FOV would mean that for many positions the receiver would not be able to detect signals from enough transmitters to achieve accurate positioning. A solution to this problem is the angular diversity aperture (ADA) receiver [14], [15].

In this paper, we describe a new form of ADA receiver specifically designed for VLP. This receiver needs only a single receiving element due to its novel use of a quadrant PD with an aperture.

Section II provides a detailed system description, initially discussing aperture receivers, followed by quadrant PDs and finally the combination of the two into a novel receiver design. Section III describes the position detection algorithm that is used and Section IV demonstrates the performance of the receiver in the presence of noise. A discussion follows in Section V and finally the conclusion in Section VI.

978-1-5386-3920-7/17/$31.00 ©2017 IEEE

II. System Description

The new AOA detector combines two key components – an aperture and a quadrant PD. The important aspects of each of these are described in this section. We have previously shown how the combination of an aperture and a PD can be used to create a directional optical receiving element and how multiple apertures and PDs can be used to design a multiple input ADA receiver. Multiple aperture ADA receivers have been shown to be very effective in both VLP applications [10] and in MIMO VLC systems [15]. In this paper, we show how a single aperture positioned above a quadrant PD can be used to create an AOA detector.

A. Aperture receivers

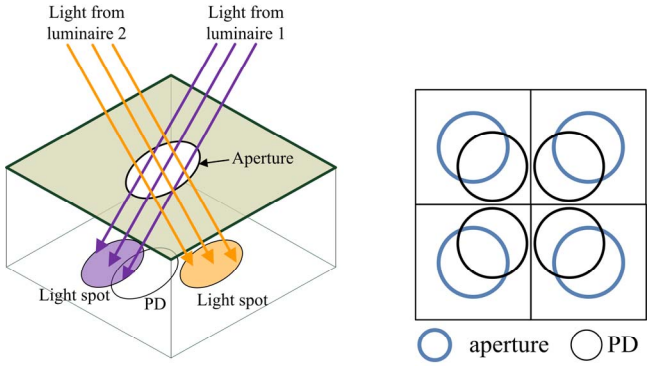

Fig. 1 Structure of the optical ADA receiver, (a) a single RE, (b), Top view of the ADA receiver with four REs

Fig. 1(a) shows a single receiving element as used in a conventional aperture receiver. Each receiving element consists of a PD and a transparent aperture in an opaque screen. The directionality of a single RE is demonstrated by considering the effect of light emitted from two different luminaires[1]. Consider light from luminaire 1. (For clarity, this is shown as purple on the figure but the color of the light is not significant.). The light creates a spot which partially overlaps with the PD. The current output from the PD is proportional to the area of overlap. Light from the other ('orange') luminaire also creates a spot of light, but as this does not overlap with the PD it is not detected. Thus, the output of the PD depends on the angle of arrival of the light. Fig. 1(b) shows how four of these receiving elements can be combined to create a multiple input receiver. In Fig. 1, round apertures and PDs are depicted, however, different shapes can be used. In this paper, we show that, for AOA estimation, it is advantageous to use a square aperture and square PD.

B. Quadrant photodiodes

Quadrant, or segmented, PDs consist of four active areas separated by a very narrow gap. These detectors are normally used in conjunction with a laser beam. As can be seen from Fig. 2, the PD is aligned so that the laser spot falls on the intersection between the quadrants. By detection of the relative photocurrents produced by each segment, any deflection in the laser beam can be accurately measured.

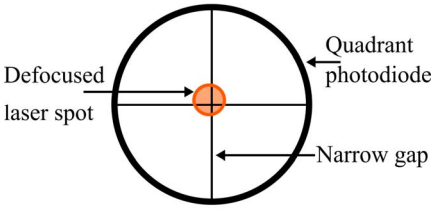

Fig. 2 Quadrant PD with small laser light spot overlapping all quadrants

Such an arrangement is widely used in atomic force microscopy [16]. Another example of widespread usage is in optical trapping [17], [18]. The common features of these systems are the use of the quadrant PD to track the movement of a beam of laser light, the size of the light spot cast is considerably smaller than the outer diameter of the receiver, and the spot shape is usually circular. Additionally, unlike our new detector design, none of these past applications use an aperture.

C. Receiver design

The receiver, shown in Fig. 3, consists of a quadrant PD located on a plane directly below an aperture that has been created in an opaque screen. The aperture plane is separated from the quadrant PD plane by a vertical distance, h. In contrast to an aperture receiver that uses conventional PDs, there is no additional benefit to a lateral offset between the aperture and the quadrant PD. Light, emitted from the LED luminaires, passes through the aperture and casts a light spot on the quadrant PD. Given knowledge of the aperture height, h, and the displacement of the light spot from the center of the quadrant PD, the AOA of the incident light can be determined.

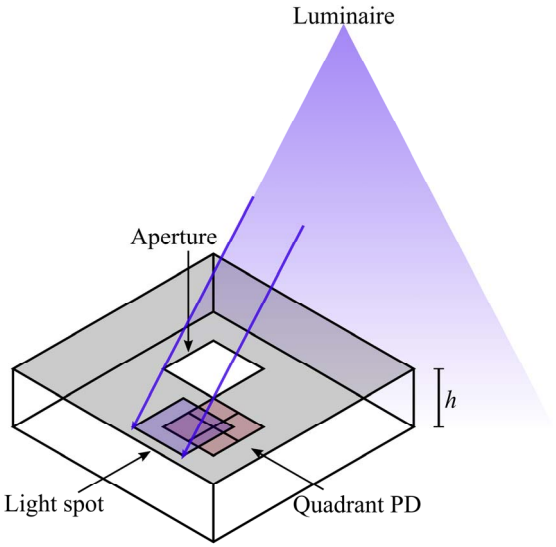

Fig. 3 Aperture receiver using a square quadrant photodiode

[1] The technical term for a light fitting is a 'luminaire'. We use this in preference to the terms 'light' or 'LED' because of the multiple meanings of 'light' and the fact that a single luminaire can be made of one or multiple LEDs

In contrast to typical quadrant PD applications, here, there is a freedom to optimize the light spot shape. The light source, primarily for room lighting, is omnidirectional. In order to cast a light spot on the quadrant photodiode, an aperture is used, the design of which can be chosen to create the desired spot shape and size. In general, for a quadrant PD, the light spot need only be larger than the gap separating the quadrants for position information to be available. However, in this receiver design, it is optimal to match the light spot to the size of the quadrant PD. A smaller aperture reduces signal strength and restricts the FOV because the light spot overlaps all four quadrants of the PD for a smaller range of arrival angles. A larger aperture leads to ambiguous results as multiple arrival angles can yield identical outputs.

In addition, by combining a square shaped aperture with a square quadrant PD, the overlap area in each quadrant changes linearly with the movement of the light spot across the PD [19]. This simplifies the algorithm required to determine incident angle from the measured photocurrents.

III. Position Detection Algorithm

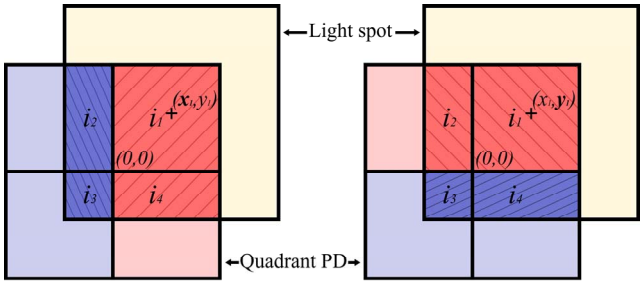

Fig. 4 Quadrant photodiodes with light spots overlapping. In (a), displacement in x is indicated by the ratio of the top and bottom quadrant pairs. In (b), displacement in y indicated by the ratio of the left and right quadrant pairs

In this section, we discuss the algorithm used to detect the position of the light spot center. In general, if the receiver is in motion, the position of the light spot will be time varying. Let $[x_1(t), y_1(t)]$ be the position at time, t. The algorithm is introduced by analyzing $x_1(t)$, and this is later extended to include both $x_1(t)$ and $y_1(t)$. The light spot center can be determined using a ratio between the photocurrents in adjacent pairs of quadrants. The photocurrent generated in each quadrant depends on the received optical power, which in turn, depends on the area of the overlap. In Fig. 4(a), $x_1(t)$ is determined by the ratio, $p_x(t)$, between the currents in the left and right quadrant pairs. This is expressed in (1), where $i_j(t)$ and $N_j(t)$ are the photocurrent and noise at time, t, received by the j^{th} quadrant of the PD, after filtering. Similarly, in Fig. 4(b), $y_1(t)$ is determined by the ratio, $p_y(t)$, between currents in the top and bottom quadrant pairs, as expressed in (2).

$$p_x(t) = \frac{i_1(t) + i_4(t) + N_1(t) + N_4(t)}{i_2(t) + i_3(t) + N_2(t) + N_3(t)} \tag{1}$$

$$p_y(t) = \frac{i_1(t) + i_2(t) + N_1(t) + N_2(t)}{i_3(t) + i_4(t) + N_3(t) + N_4(t)} \tag{2}$$

We first consider the algorithm in the absence of noise. The functions (1) and (2) reduce to a ratio of quadrant area overlaps, shown in (3), and an estimator for $x_1(t)$, or $y_1(t)$, can be derived.

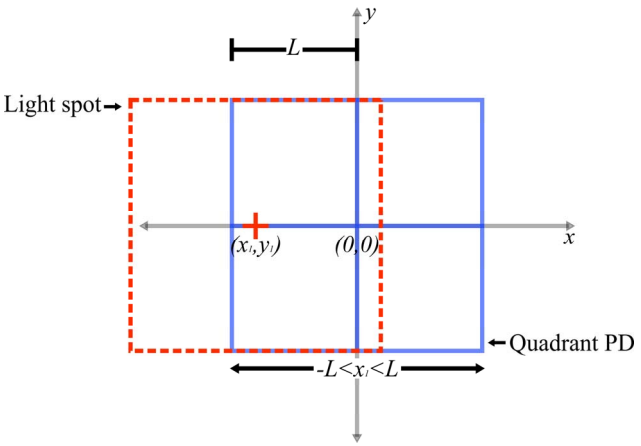

Fig. 5 Light spot, shown with dashed lines, passing over the quadrant

Initially, we will restrict the analysis to the case where the light spot passes horizontally over the quadrant PD from left to right when $y_1(t) = 0$, as shown in Fig. 5. The ratio of the overlap areas can be simplified to

$$p_x(t) = \frac{A_1(t) + A_4(t)}{A_2(t) + A_3(t)} = \begin{cases} \dfrac{2L^2 + 2Lx_1(t)}{2L^2}, & -L < x_1(t) \le 0 \\ \dfrac{2L^2}{2L^2 - 2Lx_1(t)}, & 0 < x_1(t) < L \end{cases} = \begin{cases} \dfrac{L + x_1(t)}{L}, & -L < x_1(t) \le 0 \\ \dfrac{L}{L - x_1(t)}, & 0 < x_1(t) < L \end{cases} \tag{3}$$

where $A_j(t)$ is the overlap area of the j^{th} quadrant, L is the length of a single PD quadrant and $x_1(t)$ is the x co-ordinate of the light spot center. Only values of $x_1(t)$ that result in the light spot overlapping all four quadrants are considered. For a typical case where aperture height is equal to PD length, this leads to a FOV ranging from -45° to 45°. Due to symmetry, this function is unaffected by the value of $y_1(t)$. However, the photocurrents are not independent of $y_1(t)$ as they are proportional to the overlap area. Thus, from (1), it can be seen that the signal to noise ratio (SNR) will be reduced when $y_1(t)$ is not equal to zero.

Rearranging (3) gives

$$x_1(t)=\begin{cases} L\left(p_x(t)-1\right), & -L<x_1(t)\le 0 \\ L-\dfrac{L}{p_x(t)}, & 0<x_1(t)<L \end{cases} \tag{4}$$

In (4) we derive an estimate for $x_1(t)$ from the ratio of received powers. We consider the case where low pass filtering in the electrical domain limits the bandwidth of the received signal to bandwidth B hertz. The filtered signal is then sampled at the Nyquist rate, $2B$. The estimate, at time $t=\left(k+M\right)/2B$, is then based on the average of a sequence of M samples as shown in (5). As we will show later, the statistical properties of the estimator depend on the length of this window and on the bandwidths of the optical and electrical filters at the input to the receiver.

$$\hat{x}_1\left[\frac{k+m}{2B}\right]=\begin{cases} \dfrac{1}{M}\displaystyle\sum_{n=k}^{k+M-1} L\left(p_x\left[\frac{n}{2B}\right]-1\right), & -L<x_1\left(\frac{k+m}{2B}\right)\le 0 \\ \dfrac{1}{M}\displaystyle\sum_{n=k}^{k+M-1} L-\frac{L}{p_x\left[\frac{n}{2B}\right]}, & 0<x_1\left(\frac{k+m}{2B}\right)<L \end{cases} \tag{5}$$

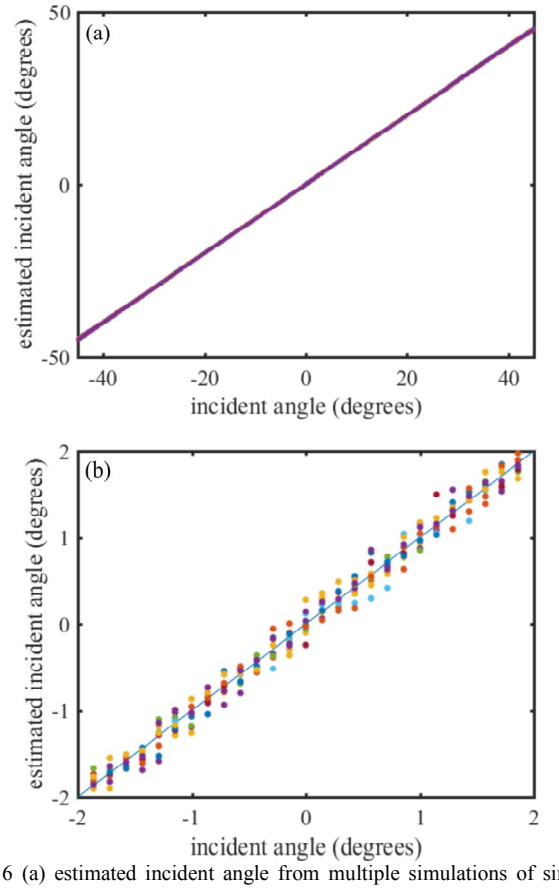

Fig. 6 (a) estimated incident angle from multiple simulations of single Nyquist samples and (b) magnification between -2 and 2 degrees

The symmetry of the receiver means that the same analysis can be applied to generate the function for $p_y(t)$ and, subsequently, $\hat{y}_1(t)$. The estimate for $\left[x_1(t), y_1(t)\right]$ can then be used, coupled with knowledge of the aperture height, to determine the incident and polar angles.

Fig. 6(a) shows an example of the estimated angle of arrival versus the actual angle for the parameters discussed in the next section. It shows that even in the presence of high levels of noise the estimated angles are in close agreement with the true incident angle for the entire FOV. Closer inspection, in Fig. 6(b), further highlights the accuracy of the estimated angle. Each spot represents the estimation from a single Nyquist rate sample, thus if multiple samples were captured, there would be an improvement in the performance. The effect of noise is discussed further in the following section.

IV. Analysis and Simulations in the Presence of Noise

In this section, we will consider the effect of noise on the algorithm and present simulation results. The noise and photocurrents are calculated using properties and dimensions of both the transmitting luminaire and quadrant PDs, combined with the position of the receiver.

The photocurrent generated by a PD can be expressed as

$$\begin{aligned} i_i(t) &= RP_R \\ &= RP_T h_c(t) \end{aligned} \tag{6}$$

where R is the responsivity of the PD, P_T and P_R are the powers transmitted and received respectively and $h_c(t)$ is the DC channel gain. For simplicity, we consider the typical VLP case where the incidence and emergence angles are equal and the Lambertian order of the LED is 1. Changes to these values will change the absolute received powers, however will not change the ratio. The DC channel gain is then given by

$$h_c(t)=\frac{A_i(t)}{\pi d^2}\cos^2\left(\psi(t)\right) \tag{7}$$

The distance from the LED transmitter to the receiver is $d=\left(H+h\right)/\cos\left(\psi(t)\right)$, $\psi(t)=\arctan\left(\sqrt{x_1(t)^2+y_1(t)^2}\,/h\right)$ is the incident angle, h is the vertical height from the PD to the aperture and H is the vertical height from the receiver to the transmitter.

We consider only the dominant noise source, which is the shot noise induced by background illumination. This is modelled as white Gaussian noise with single sided power density given by

$$N_0=2qRp_nA\Delta\lambda \tag{8}$$

where q is the charge of an electron, R is the responsivity of the PD, p_n is the spectral irradiance, A is the area of one PD quadrant, $\Delta\lambda$ is the bandwidth of the optical filter. The variance is then given by

$$\sigma_n^2 = N_0 B \tag{9}$$

where B is the bandwidth of the electrical filter. Unlike the received optical power signal, the noise is added in the electrical domain and is thus bipolar. This variance will be an over estimate as the receiver is directional and the opaque screen will block some of the ambient light. Simulation parameters can be seen in Table 1.

TABLE 1 SIMULATION PARAMETERS

Parameter	Value
Power transmitted (P_T)	3 W
Responsivity (R)	0.65 A/W
Optical filter bandwidth $(\Delta\lambda)$	300 nm
Electrical filter bandwidth (B)	1 MHz
Spectral irradiance (p_n)	6.2 x 10^{-6} W/(nm.cm^2)

In the presence of noise, the function previously described in (3) now becomes

$$p_x(t) = \begin{cases} \dfrac{2k_1\cos^4(\psi(t))L^2 + 2k_1\cos^4(\psi(t))Lx_1(t) + N_1(t) + N_4(t)}{2k_1\cos^4(\psi(t))L^2 + N_2(t) + N_3(t)} \\ \quad = \dfrac{L + x_1(t) + E_1(t)}{L + E_2(t)}, \quad -L < x_1(t) \le 0 \\ \dfrac{2k_1\cos^4(\psi(t))L^2 + N_1(t) + N_4(t)}{2k_1\cos^4(\psi(t))L^2 - 2k_1\cos^4(\psi(t))Lx_1(t) + N_2(t) + N_3(t)} \\ \quad = \dfrac{L + E_1(t)}{L - x_1(t) + E_2(t)}, \quad 0 < x_1(t) < L \end{cases} \tag{10}$$

$E_1(t)$ and $E_2(t)$ have a normal distribution with zero mean and variance $\sigma_e(t)^2$ given by

$$\begin{aligned} \sigma_e(t)^2 &= \left(\frac{1}{2k_1\cos^4(\psi(t))L}\right)^2 \times 2\sigma_n^2 \\ &= \frac{\pi^2(H+h)^4 qp_n\Delta\lambda B}{RP_T^2\cos^8\left(\arctan\left(\sqrt{x_1(t)^2 + y_1(t)^2}/h\right)\right)} \end{aligned} \tag{11}$$

The magnitude of the variance is dependent on multiple variables. It is directly proportional to the optical and electrical bandwidths and inversely proportional the square of the transmitted power. The $\cos^8(\psi(t))$ term is related to the geometry of the receiver and, depending on the ratio of the PD length to the aperture height, has substantial effects on the root mean square error curve. Fig. 7 shows the root mean square error of the estimate for the case where only a single sample is used, i.e. $M = 1$. For the worst case, where $h = 0.5L$, the root mean square error in the angle is less than 1 degree and much smaller for the majority of the incident angles. As the aperture height increases, the root mean square error decreases dramatically, however the receiver FOV also decreases and the receiver becomes more bulky. In photography, a similar phenomenon called natural vignetting is seen where the

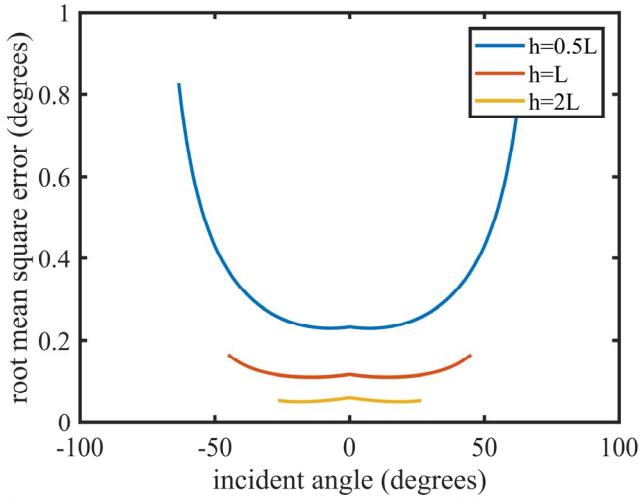

Fig. 7 Root mean square error for varying aperture height

illumination is dependent of the fourth power of the cosine of the incident angle and the geometry of the system. [20].

In Fig. 8, we keep the PD length equal to the aperture height, $h = L$, so that we can see the effect of increasing the PD area. Although the variance in (11) is not directly dependent on the area of the PD, as the PD becomes larger, the error in the detection of the light spot center, $[x_1(t), y_1(t)]$, will remain constant and thus an increased PD size will result in increased accuracy. This can be seen in Fig. 8 where the root mean square error in arrival angle detection is shown for increasing PD length, and thus area. Significant improvements can be gained by increasing the PD area, however it will also increase the overall size of the receiver. Typical off the shelf quadrant PDs can have an area of up to 100mm^2, thus it is practical to choose a quadrant PD around this size.

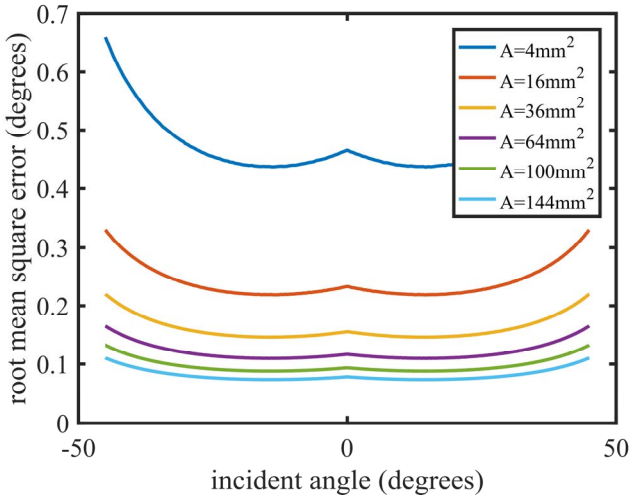

Fig. 8 Root mean square error for varying PD area

V. DISCUSSION

The results show that the new AOA detector can provide accurate angle of arrival estimation. The simulation results

which have been presented are for the case of one transmitter, and to simplify the description of the new technique are based on the dc component of the optical power received from that transmitter. In practice it would be better to use a modulated signal as this would allow any dc component due to background light to be eliminated. In the case of a modulated signal the estimate should be based on the output of a matched filter, which is matched to the known transmitted signal. In this case the accuracy of the estimate depends on the SNR at the output of the matched filter. The technique can readily be extended to calculating the AOA for signals from multiple transmitters. To do this the transmitters should transmit orthogonal signals. As long as orthogonal signals are used, single quadrature detector can be used to simultaneously estimate multiple AOAs, by using multiple matched filters each matched to one of the orthogonal signals,

The simulations show that very accurate estimates can be made based on a single sample. However if necessary the robustness in the presence of noise can be improved by using an average of the samples rather than a single sample for the estimate. As the position of the receiver in a typical indoor application will not change rapidly, estimates can be based on multiple samples taken over a relatively long time (e.g. ms).

In practice the accuracy of position estimation may be limited by other factors, such as the size and shape of luminaires, slight imbalances in the properties of the four quadrants of the PD, and if the aperture or PD is not perfectly square or it the aperture and PD are not perfectly aligned. These effects will be the subject of future research.

VI. Conclusion

This paper has presented a novel detector for visible light positioning. The new receiver combines an aperture with a quadrant PD. It is shown that the position of the spot of light on the quadrant PD caused by light passing through the aperture gives information about the position of the receiver relative to the transmitter. A new angle of arrival estimation algorithm is presented which uses the relative received power in each quadrant to estimate the direction of the received light. Analytical and simulation results are presented which show that for a square aperture and a square photodiode the x and y coordinates of the receiver can be separately estimated. The properties of the new estimator in the presence of noise are analyzed. It is shown that the variance of the estimates is smallest when the transmitting luminaire is directly above the receiver and increases as the offset between transmitter and receiver increases. This is because of the reduced received optical power as the angle of incidence of light on the quadrant photodiode increases. It is shown that the variance of the estimator depends on the bandwidths of the optical and electrical filters at the receiver front end, and on the time integration window used. Long integration time windows are possible in typical VLP positioning applications as receivers are typically stationary or moving very slowly. The new receiver can be used to simultaneously detect position relative to a number of transmitters as long as the transmitters transmit known orthogonal signals. No extra apertures or photodetectors are required. In this case the position of the receiver can be calculated using triangulation or trilateration.

Acknowledgment

This work was supported by the Australian Research Council's (ARC) Discovery funding scheme (DP150100003)

References

[1] J. Armstrong, Y. A. Sekercioglu, and A. Neild, 'Visible light positioning: a roadmap for international standardization', *IEEE Commun. Mag.*, vol. 51, no. 12, pp. 68–73, Dec. 2013.

[2] T. Komine and M. Nakagawa, 'Fundamental analysis for visible-light communication system using LED lights', *IEEE Trans. Consum. Electron.*, vol. 50, no. 1, pp. 100–107, Feb. 2004.

[3] Y.-S. Kuo, P. Pannuto, K.-J. Hsiao, and P. Dutta, 'Luxapose: indoor positioning with mobile phones and visible light', in *Proc. of the Annual International Conference on Mobile Computing and Networking,* Maui, United States, 2014, pp. 447–458.

[4] L. Li, P. Hu, C. Peng, G. Shen, and F. Zhao, 'Epsilon: A Visible Light Based Positioning System', in *Proceedings of the 11th USENIX Symposium on Networked Systems Design and Implementation*, Berkeley, Calif, 2014, pp. 331–343.

[5] T.-H. Do and M. Yoo, 'An in-Depth Survey of Visible Light Communication Based Positioning Systems', *Sensors*, vol. 16, no. 5, May 2016.

[6] W. Gu, W. Zhang, M. Kavehrad, and L. Feng, 'Three-dimensional light positioning algorithm with filtering techniques for indoor environments', *Opt. Eng.*, vol. 53, no. 10, pp. 107107–107107, 2014.

[7] T. Q. Wang, Y. A. Sekercioglu, A. Neild, and J. Armstrong, 'Position Accuracy of Time-of-Arrival Based Ranging Using Visible Light With Application in Indoor Localization Systems', *J. Light. Technol.*, vol. 31, no. 20, pp. 3302–3308, Oct. 2013.

[8] K. Panta and J. Armstrong, 'Indoor localisation using white LEDs', *Electron. Lett.*, vol. 48, no. 4, pp. 228–230, Feb. 2012.

[9] A. M. Vegni and M. Biagi, 'An indoor localization algorithm in a small-cell LED-based lighting system', in *2012 International Conf. on Indoor Positioning and Indoor Navigation (IPIN)*, 2012, pp. 1–7.

[10] H. Steendam, T. Q. Wang, and J. Armstrong, 'Theoretical Lower Bound for Indoor Visible Light Positioning Using Received Signal Strength Measurements and an Aperture-Based Receiver', *J. Light. Technol.*, vol. PP, no. 99, pp. 1–1, 2016.

[11] G. del Campo-Jimenez, J. M. Perandones, and F. J. Lopez-Hernandez, 'A VLC-based beacon location system for mobile applications', in *2013 International Conference on Localization and GNSS (ICL-GNSS)*, 2013, pp. 1–4.

[12] S. H. Yang, H. S. Kim, Y. H. Son, and S. K. Han, 'Three-Dimensional Visible Light Indoor Localization Using AOA and RSS With Multiple Optical Receivers', *J. Light. Technol.*, vol. 32, no. 14, pp. 2480–2485, Jul. 2014.

[13] L. Wei, H. Zhang, B. Yu, J. Song, and Y. Guan, 'Cubic-Receiver-Based Indoor Optical Wireless Location System', *IEEE Photonics J.*, vol. 8, no. 1, pp. 1–7, Feb. 2016.

[14] T. Q. Wang, C. He, and J. Armstrong, 'Angular diversity for indoor MIMO optical wireless communications', in *2015 IEEE Int. Conf. on Communications (ICC)*, 2015, pp. 5066–5071.

[15] T. Q. Wang, C. He, and J. Armstrong, 'Performance Analysis of Aperture-Based Receivers for MIMO IM/DD Visible Light Communications', *J. Light. Technol.*, vol. PP, no. 99, pp. 1–1, 2016.

[16] S. Alexander et al., 'An atomic-resolution atomic-force microscope implemented using an optical lever', *J. Appl. Phys.*, vol. 65, no. 1, pp. 164–167, Jan. 1989.

[17] S. Keen, J. Leach, G. Gibson, and M. J. Padgett, 'Comparison of a high-speed camera and a quadrant detector for measuring displacements in optical tweezers', *J. Opt. Pure Appl. Opt.*, vol. 9, no. 8, p. S264, 2007.

[18] S. Lakämper, A. Lamprecht, I. A. T. Schaap, and J. Dual, 'Direct 2D measurement of time-averaged forces and pressure amplitudes in acoustophoretic devices using optical trapping', *Lab. Chip*, vol. 15, no. 1, pp. 290–300, Dec. 2014.

[19] 'Quadrant and Bi-Cell Silicon Photodiode Amplifier Module'. OSI Optoelectronics.

[20] Ray, Sidney F., *Applied Photographic Optics,* 2nd edition. Oxford: Focal Press, 1994